Available online at www.sciencedirect.com
SCIENCE DIRECT®
PERGAMON
Polyhedron 22 (2003) 3025–3035
POLYHEDRON
www.elsevier.com/locate/poly

Structural and magnetic properties of three copper(II) pyridine-2,3-dicarboxylate coordination polymers incorporating the same chain motif

Brian O. Patrick, Cecilia L. Stevens, Alan Storr *, Robert C. Thompson *

Department of Chemistry, The University of British Columbia, Vancouver, BC, Canada V6T 1Z1

Received 20 June 2002; accepted 28 September 2002

Abstract

The complex $[Cu(2,3\text{-pydcH})_2]$, (**1**), ($2,3\text{-pydcH}_2 = 2,3$-pyridinedicarboxylic acid) is a chain polymer. Two ligands occupy the equatorial plane of each tetragonally elongated octahedral Cu^{2+} coordination sphere, chelating through the pyridine nitrogen and one oxygen of the deprotonated 2-carboxylic acid group; the axial positions are occupied by long bonds to a 3-carboxylic acid oxygen of adjacent $Cu(2,3\text{-pydcH})_2$ repeat units. This polymeric chain motif also appears in two heterometallic complexes incorporating the doubly deprotonated dicarboxylate ligand species 2,3-pydc; namely $[Cu(2,3\text{-pydc})_2][Na_2(H_2O)_6(\mu\text{-}H_2O)_2]$, (**2**), and $[Cu(2,3\text{-pydc})_2][Mn(H_2O)_6]\cdot 2H_2O$, (**3**). In **2**, the chains are cross-linked via a novel disodium cation $[Na_2(H_2O)_6(\mu\text{-}H_2O)_2]^{2+}$ to form a 2D sheet structure. In **3**, the chains carry a formal 2− charge per copper centre, with charge neutrality achieved by the presence of isolated $[Mn(H_2O)_6]^{2+}$ complex cations in the lattice. The structural and magnetic properties of these three species are compared.

Keywords: Structural and magnetic properties; Chain polymers; X-ray diffraction; Bridging ligands

1. Introduction

Previous work by this and other groups [1,2] has established mono- and di-deprotonated pyrazine-2,3-dicarboxylic acid as bridging ligands capable of forming coordination polymers with transition metals and, when the metals are paramagnetic, capable of mediating magnetic exchange through the polymeric structure. The anions of pyridine 2,3-dicarboxylic acid ($2,3\text{-pydcH}_2$) share this ability, although they have fewer possible bridging modes than the pyrazine derivatives. Indeed, constraint in the bridging modes of pyridine 2,3-dicarboxylates is evident in the studies reported here, where the same chain motif appears in three different coordination polymers. This work examines the structural and magnetic behaviour of the three polymers, $[Cu(2,3\text{-pydcH})_2]$ (**1**), $[Cu(2,3\text{-pydc})_2][Na_2(H_2O)_6(\mu\text{-}H_2O)_2]$ (**2**), and $[Cu(2,3\text{-pydc})_2][Mn(H_2O)_6]\cdot 2H_2O$ (**3**). The structures of **1** and **2** reported earlier [3,4] are reexamined here at lower temperatures, while that of **3** is reported here for the first time.

2. Experimental

2.1. Syntheses

2,3-Pyridine dicarboxylic acid ($2,3\text{-pydcH}_2$) (Aldrich), $Cu(NO_3)_2\cdot 3H_2O$ (Baker), $Cu(CH_3COO)_2\cdot H_2O$ (BDH), and $MnCl_2\cdot 4H_2O$ (Fisher) were used as supplied. Water was deionised in-house.

$[Cu(2,3\text{-pydcH})_2]$ (**1**), was prepared by dissolving $2,3\text{-pydcH}_2$ (2.5 mmol, 0.42 g) in 900 ml H_2O and adding a solution of $Cu(CH_3COO)_2\cdot H_2O$ (1.25 mmol,

* Corresponding authors. Tel.: +1-604-822-3962; fax: +1-604-822-2847 (Alan Storr), Tel.: +1-604-822-4979; fax: +1-604-822-2847 (Robert C. Thompson).

E-mail addresses: storr@chem.ubc.ca (A. Storr), thompson@chem.ubc.ca (R.C. Thompson).

0277-5387/$ - see front matter © 2003 Elsevier Ltd. All rights reserved.
doi:10.1016/S0277-5387(03)00433-9

0.25 g) in 100 ml H_2O. The solution turned pale blue upon mixing. After three weeks, the solution was filtered to obtain small blue needles large enough for single-crystal X-ray studies. *Anal.* Found: C, 42.3; H, 2.0; N, 6.9. Calc. for $CuC_{14}H_8N_2O_8$, C, 42.5; H, 2.0; N, 7.1%. This preparation differs somewhat from that reported earlier [4].

$Cu(2,3\text{-pydc})_2][Na_2(H_2O)_6(\mu\text{-}H_2O)_2]$ (**2**). Exploring a synthetic procedure similar to that described earlier [3], 2,3-pydcH$_2$ (1.0 mmol, 0.167 g) was taken up in H_2O and 2.5 mmol NaOH (25.00 ml 0.10 M solution) added, to a final volume of ~100 ml. $Cu(NO_3)_2 \cdot 6H_2O$ (0.50 mmol in a few ml H_2O) was added and the reaction mixture immediately turned deep royal blue. This was left to evaporate to dryness, leaving rectangular royal-blue prisms interspersed with small white crystals. The residue was washed with ice-cold methanol, leaving a pale blue powder which was then taken up in water and again evaporated to dryness, to obtain royal blue needles of **2** suitable for single-crystal X-ray diffraction in 64% isolated yield. *Anal.* Found: C, 29.1 H, 3.8; N, 4.6. Calc. for $CuNa_2C_{14}H_{22}N_2O_{16}$: C, 28.8; H, 3.8; N, 4.8%.

$[Cu(2,3\text{-pydc})_2][Mn(H_2O)_6] \cdot 2H_2O$ (**3**). A solution was prepared of 0.1 mmol $[Cu(2,3\text{-pydc})_2][Na_2(H_2O)_6(\mu\text{-}H_2O)_2]$ (**2**), in ~5 ml H_2O. This was added to a solution of $MnCl_2 \cdot 4H_2O$ (0.1 mmol, 0.020 g) in ~5 ml H_2O. Blue crystals appeared after one week and the reaction mixture was filtered one week later to obtain bright blue blocks of **3** in 75% isolated yield. *Anal.* Found: C, 28.6; H, 3.7; N, 4.8. Calc. for $CuMnC_{14}H_{22}N_2O_{16}$: C, 28.4; H, 3.7; N, 4.7%.

2.2. Physical measurements

TGA data were recorded on a TA 51 thermogravimetric analyser at a 10 °C/min. ramp under an 100 cc/min stream of nitrogen. DC magnetic susceptibilities were measured using a Quantum Design (MPMS) SQUID magnetometer. Measurements were taken at 10,000 G over the temperature range 300–2 K. The sample holder and details regarding the use of the equipment have been described elsewhere [5]. Magnetic susceptibilities were corrected for background signal of the sample holder. Corrections for the diamagnetism of all atoms came to -160×10^{-6} for **1**, -254×10^{-6} for **2**, and -258×10^{-6} for **3**. All magnetic measurements were done on finely powdered samples and the data are reported here on a per mole copper basis. X-ray studies were performed on single crystals mounted on glass fibres. All measurements were made on a Rigaku/ASDC CCD area detector with graphite monochromated Mo Kα radiation. The positions of hydrogen atoms bonded to carbon were calculated, while those bonded to oxygen were located by electron density.

3. Results and discussion

3.1. [Cu(2,3-pydcH)$_2$] (1)

TGA analysis showed that **1** remains stable until 280 °C, at which temperature the ligand decomposes.

From a high-dilution synthesis, crystals suitable for single-crystal X-ray diffraction studies were obtained. Crystallographic data are given in Table 1 and a view of the repeat unit with atom numbering is shown in Fig. 1. The earlier structural determination was done at 296 K [4], while the data reported here were obtained at 173 K. The structure is essentially the same at the two temperatures. However, cell dimensions are expected to decrease slightly at lower temperatures and while this was observed for *b* and *c*, interestingly, *a* at 173 K (6.754(1) Å) is actually longer than at 296 K (6.730(3) Å). As expected, the unit cell volume has decreased, from 685.3(3) Å^3 at 296 K to 680.0(2) Å^3 at 173 K. Differences in bond parameters involving copper are seen at the two different temperatures. Most notable are: (i) the Cu–O4 distances decrease from 2.660(3) Å at 296 K [4] to 2.616(3) Å at 173 K, (ii) the O1–Cu–O4 bond angle is 84.9(1)° at 296 K [4] and 90.0(2)° at 173 K and (iii) the O1–Cu–N angle is 88.8(1)° at 296 K [4] and 83.7(1)° at 173 K. In the discussion of the structure below, the data from our 173 K determination are used.

The structure is in many respects similar to that of the analogous pyrazine-2,3-dicarboxylate compound, $[Cu(pyzdcH)_2] \cdot 2H_2O$ [1]. Each Cu^{2+} ion has a tetragonally distorted octahedral coordination sphere. The equatorial plane is occupied by two 2,3-pydcH ligands coordinating through the pyridine nitrogen and one oxygen of the deprotonated 2-carboxyl group, with re-

Table 1
Crystallographic data for **1**

Empirical formula	$C_{14}H_8N_2O_8Cu$
Formula weight	395.77
Crystal system	monoclinic
Space group	$P2_1/n$(#14)
a (Å)	6.754(1)
b (Å)	12.864(2)
c (Å)	8.197(1)
β (°)	107.28(1)
V (Å^3)	680.0(2)
Z	2
ρ_{calc} (g cm^{-3})	1.933
μ(Mo Kα) (cm^{-1})	16.6
Crystal size (mm)	0.30 × 0.10 × 0.05
T (K)	173
$R(F)^*$	0.034
$R_W(F^2)^¥$	0.104
Number of parameters	119
Refinement	F^2

$^*R(F) = \sum ||F_o| - |F_c|| / \sum |F_o|$.
$^¥R_W(F^2) = (\sum (F_o^2 - F_c^2)^2 / \sum (F_o^2)^2)^{1/2}$.

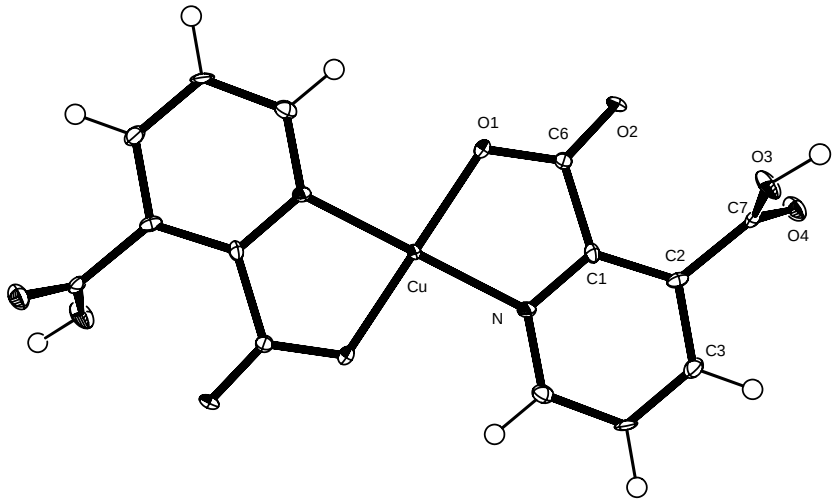

Fig. 1. Repeat unit of **1**, with atom numbering scheme (50% ellipsoids).

spective bond lengths of 1.973(3) and 1.934(3) Å, which are comparable to the corresponding Cu–N and Cu–O lengths (1.996(2) and 1.948(1) Å, respectively) in $[Cu(pyzdcH)_2]\cdot 2H_2O$ [1]. The axial positions of the Cu^{2+} coordination sphere are occupied by long bonds (2.616(3) Å, compared to the published value of 2.405(2) for $[Cu(pyzdcH)_2]\cdot 2H_2O$ [1]) to the nonprotonated oxygen of the 3-carboxyl group on adjacent repeat units, resulting in a double bridge linking the copper centres into a chain polymer (Fig. 2). These polymeric chains are further linked by intermolecular contacts. As previously reported [4], the proton on the carboxylic acid group of one chain approaches the 2-carboxyl oxygen not bound to copper (II) in the adjacent chain, with an O–O distance of 2.633 Å and an OH–O distance of 1.752 Å. This structure has been further examined here by an analysis of π–π interactions. In ligating the adjacent copper centre, the 3-carboxylic acid group twists at an angle of 73.05° to the plane of the pyridine ring (see Table 2 for selected bond lengths and angles). The pyridine rings all lie parallel to each other, and the overlapping pyridine rings of adjacent polymer repeat units within the chain have a centroid–centroid distance of 4.593 Å, with an angle of 43.42° between the centroid–centroid and plane normal vectors (Fig. 2). This gives a ring offset of 3.157 Å and also places the nonligating 2-CO_2 oxygen of each 2,3-pydcH almost directly over the centroid of the other ring. The 2-CO_2 group is twisted at an angle of 7.11° to the pyridine ring, such that although the ring planes are 3.336 Å apart each O2

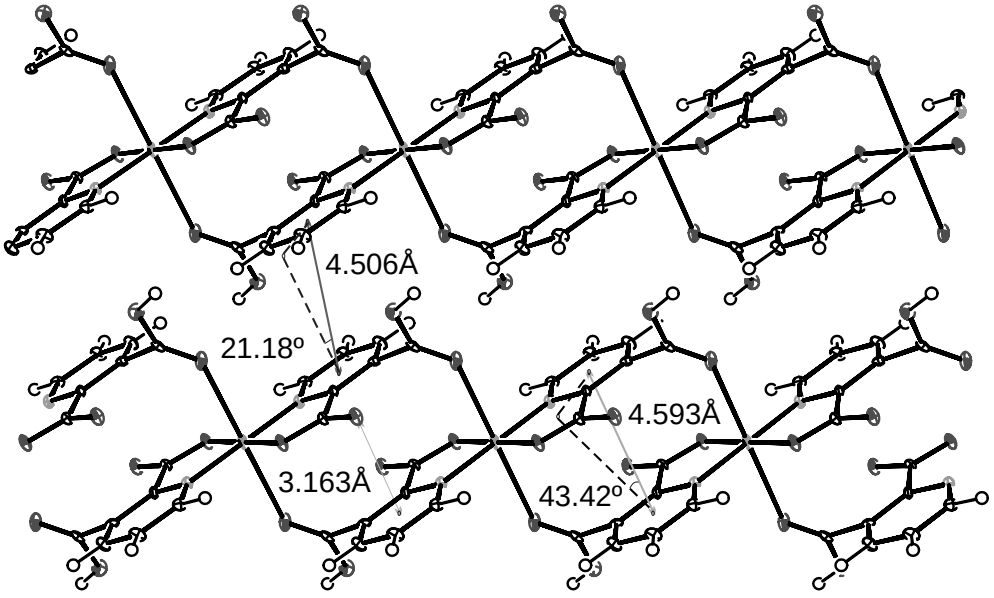

Fig. 2. View of a section of the extended structure of **1**, showing π–π interactions.

Table 2
Selected bond lengths and distances (Å), and angles (°) for **1**

Bond lengths	
Cu–N	1.973(3)
Cu–O1	1.934(3)
Cu–O4	2.616(3)
Bond angles	
O1–Cu–N	83.7(1)
O1–Cu–O4	90.0(2)
Torsion angles	
C1–C2–C3–O1–C6–O2	7.11
C1–C2–C3–O3–C7–O4	73.05
Centroid–centroid distance (adjacent repeat units)	4.593
Ring plane–ring plane distance (adjacent repeat units)	3.336
Centroid–centroid to ring normal angle	43.42
Ring offset	3.157
O2–centroid distance	3.163

lies only 3.163 Å from the neighbouring ring centroid, a geometry suggestive of π–π interactions involving the carboxylate group [6]. There are also interchain π–π interactions observed in **1** (Fig. 2). The pyridine rings of adjacent chains lie parallel to each other, with a centroid–centroid distance of 4.506 Å and an angle of 21.18° between the centroid–centroid and ring normal vectors. This results in a ring offset of 1.628 Å, a geometry consistent with π–π slipped stacking interactions [6]. These interchain interactions give **1** a novel 3D extended structure, with coordinate–covalent interaction along the chain direction, π–π stacking interactions in the second dimension, and H-bonding interactions in the third (see Fig. 3).

Magnetic susceptibility measurements were made on **1** at an applied field of 10,000 G over the temperature range 300–2 K. Susceptibility and magnetic moment plots are shown in Fig. 4. Although no maximum is observed in the susceptibility plot, the decrease in μ_{eff} at low T suggests the presence of antiferromagnetic coupling. Anticipating that any interchain coupling would be negligible compared to intrachain exchange, the data were fit to the Weng model for antiferromagnetically coupled linear chains using the Hiller coefficients for $S = 1/2$ [7,8]. Goodness of fit was measured by the least-squares fitting function

$$F = \sqrt{\frac{1}{n}\sum_{i=1}^{n}\left[\frac{\chi^i_{\text{calc}} - \chi^i_{\text{obs}}}{\chi^i_{\text{obs}}}\right]^2}.$$

A satisfactory fit ($F = 0.003$) was obtained with the parameters $J = -0.055(3)$ cm^{-1}, $g = 2.106(1)$, and a TIP correction of 0.000023(3) cm^3 mol^{-1}. This degree of antiferromagnetic exchange may be described as weak due to the lack of a maximum in the susceptibility plot above 2 K and the small coupling constant. The structurally similar species $[Cu(pyzdcH)_2]\cdot 2H_2O$ also shows antiferromagnetic activity, with the published parameters $g = 2.14$ and $J = -0.11$ cm^{-1} [1], nearly twice the corresponding value for **1**. This discrepancy is likely the result of the fact that the exchange in both compounds must be mediated via the axial Cu–O bonds, and these are significantly longer for **1** (2.616(3) Å) than for $[Cu(pyzdcH)_2]\cdot 2H_2O$ (2.405(2) Å).

3.2. *[Cu(2,3-pydc)$_2$][Na$_2$(H$_2$O)$_6$(μ-H$_2$O)$_2$], (**2**)*

An earlier thermal analysis study of **2** [3] showed the loss of water in two steps, one at 95 °C corresponding to the loss of six water molecules, followed by one at 163 °C corresponding to the loss of the other two. In our experiment, we were unable to discern this amount of detail in the thermogram; our study showed a continuous loss of weight from just above room temperature to about 190 °C, the total weight loss corresponding to the loss of eight water molecules. We observed further weight loss due to ligand decomposition at about 270 °C, consistent with the earlier thermal differential analysis results [3].

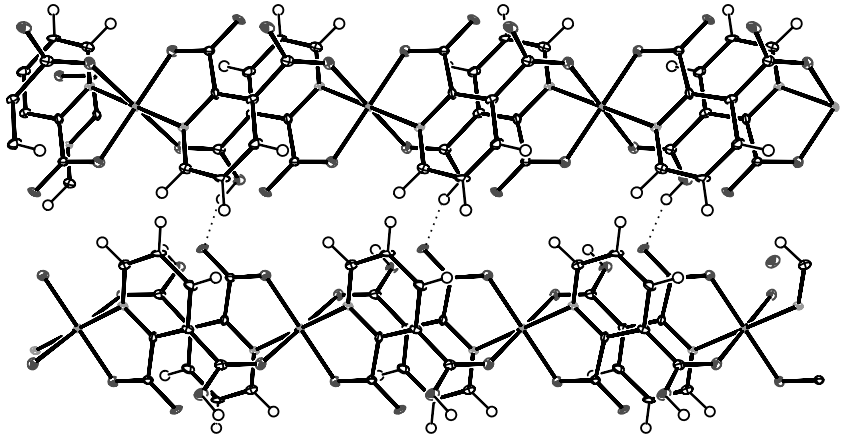

Fig. 3. View of a section of the extended structure of **1**, showing hydrogen bonding.

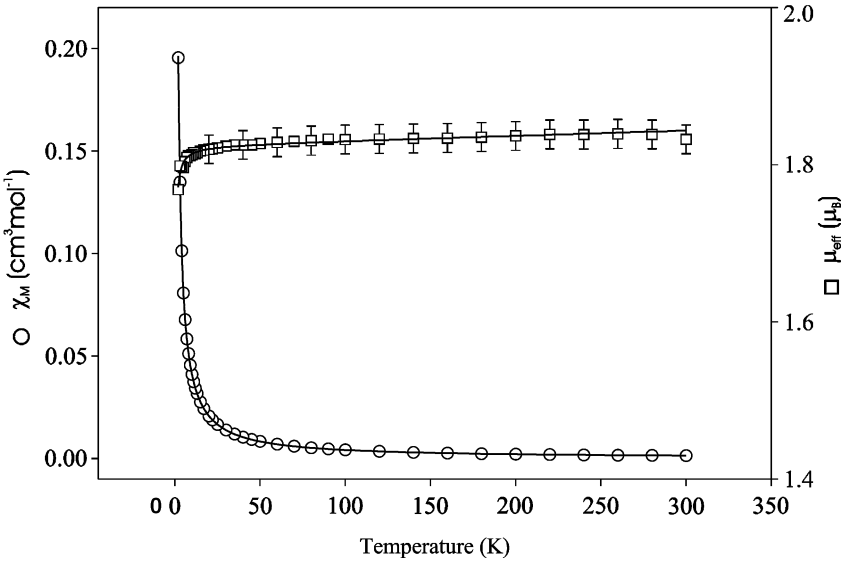

Fig. 4. χ_M and μ_{eff} vs. temperature plot for **1**, with error bars at ±0.5%. Lines are from theory as described in the text.

Comparison of the crystallographic data for **2** obtained at 173 K in this work (Table 3) with data obtained previously at 293 K [3] shows the structure to be essentially the same at the two temperatures. As for **1**, the volume decreases with temperature from 2183.3(4) Å^3 at 293 K [3] to 2171.2(3) Å^3 at 173 K, the *b* and *c* dimensions are shorter at the lower temperature while *a* increases from 21.274(1) Å at 293 K to 21.412(1) Å at 173 K. Unlike **1**, however, there are no large differences at the two temperatures in bond lengths or angles involving copper. The data obtained at 173 K in this work are used in the discussion below of the structure of **2**.

Compound **2** is formed of chains similar to **1**, albeit with both carboxyl groups deprotonated. Crystallographic data (Table 3) are substantially similar to those previously reported [3]. See Table 4 for selected bond lengths and angles; Fig. 5 shows the repeat unit with atom labelling. The 2,3-pydc bridged copper chains are cross-linked via novel disodium dications coordinated by the second oxygen of the 2-carboxylate group of each ligand. The disodium cation $[Na_2(H_2O)_6(\mu\text{-}H_2O)_2]^{2+}$ consists of two identical Na^+ ions in octahedral coordination spheres (see Fig. 6). Each sodium centre coordinates with a pyridine 2-carboxyl oxygen, and fills out its coordination sphere with three terminal H_2O ligands

Table 3
Crytallographic data for **2**

Empirical formula	$C_{14}H_{22}O_{16}N_2CuNa_2$
Formula weight	583.86
Crystal system	monoclinic
Space group	*C*2/*c*(#15)
a (Å)	21.412(1)
b (Å)	6.0967(7)
c (Å)	16.990(1)
β (°)	101.780(2)
V (Å^3)	2171.2(3)
Z	4
ρ_{calc} (g cm^{-3})	1.786
μ(Mo Kα) (cm^{-1})	11.32
Crystal size (mm)	0.25 × 0.20 × 0.15
T (K)	173
$R(F)^*$	0.027
$R_W(F^2)^¥$	0.078
Number of parameters	192
Refinement	F^2

$^* R(F) = \sum ||F_o| - |F_c|| / \sum |F_o|$.
$^¥ R_W(F^2) = (\sum(F_o^2 - F_c^2)^2 / \sum(F_o^2)^2)^{1/2}$.

Table 4
Selected bond lengths and distances (Å) and angles (°) for **2**

Bond lengths	
Cu–N	1.965(1)
Cu–O1	1.957(1)
Cu–O4	2.661(1)
Na–O2	2.335(2)
Na–O5	2.385(2)
Na–O6	2.405(2)
Na–O7	2.404(2)
Na–O7′	2.589(2)
Na–O8	2.405(2)
Bond angles	
O1–Cu–N	83.51(5)
O1–Cu–O4	80.0(2)
Torsion angles	
C1–C2–C3–O1–C6–O2	3.54
C1–C2–C3–O3–C7–O4	98.7
Centroid–centroid distance (adjacent repeat units)	4.516
Ring plane–ring plane distance (adjacent repeat units)	3.257
Centroid–centroid to ring normal angle	43.85
Ring offset	3.128
O2–centroid distance	3.503

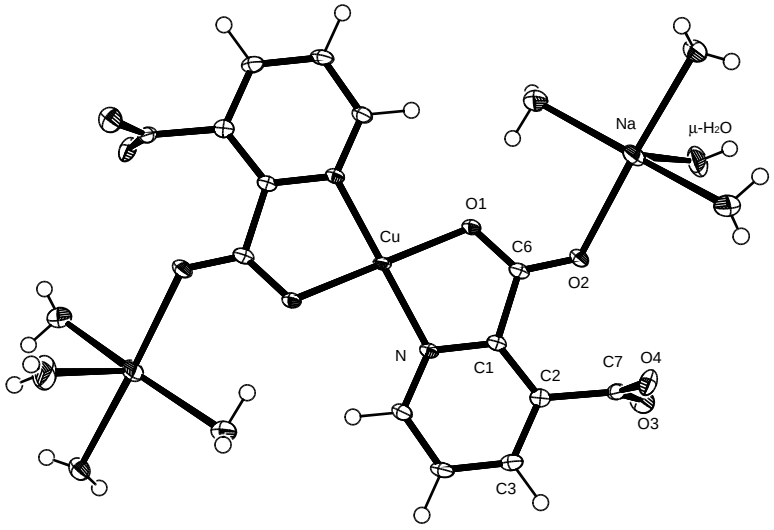

Fig. 5. Repeat unit of **2**, with atom numbering scheme (50% ellipsoids).

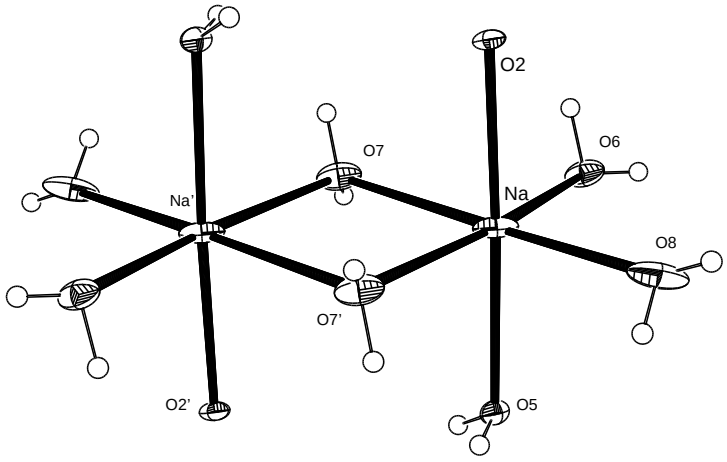

Fig. 6. View of the disodium dication, with atom numbering scheme (50% ellipsoids).

and two bridging H_2O groups. The observed bond lengths are consistent with those observed in published coordinated sodium species [9,10].

The copper coordination sphere is, in the equatorial plane, very similar to that of **1**: the Cu–N bond of **2** is slightly shorter than that of **1** (2 esd), while the Cu–O1 of **2** is slightly longer than that of **1** (6 esd). The main difference is in the axial Cu–O4 bond lengths, which in **2** are distinctly greater than in **1** (11 esd). This may be a result of the anionic character of the bridging ligands, which leads to greater ligand–ligand repulsion in the case of **2**. As in **1**, the 3-CO_2 is twisted with respect to the pyridine ring, this time by 98.7°. The pyridine rings of adjacent repeat units lie parallel, and have a centroid–centroid distance of 4.516 Å and an angle of 43.85° between the centroid–centroid and plane normal vectors, giving an offset of 3.128 Å. Again, each O2 lies centrally over the adjacent pyridine ring. The 2-CO_2 group is again slightly turned with respect to the pyridine ring, but in this case the Na^+ ion coordinatively bound to O2 lifts O2 slightly away from the adjacent pyridine ring, so that it lies 3.503 Å from the centroid – a geometry again suggestive of π–π interactions involving the carboxylate group [6]. No further π–π interactions are observed in **2**, although the water molecules coordinating the disodium dication form an extensive 3D network of hydrogen bonds. This network is described in detail in the earlier work [3]. Fig. 7 shows a portion of the polymeric sheet structure.

Magnetic susceptibility measurements for **2** (see Fig. 8 for susceptibility and moment plots) were initially analysed under the assumption that any exchange mediated by the disodium cations would be negligible in comparison with the intrachain exchange. The data were therefore fit to the Weng linear model as for **1**, and a satisfactory ($F = 0.005$) fit obtained with the parameters

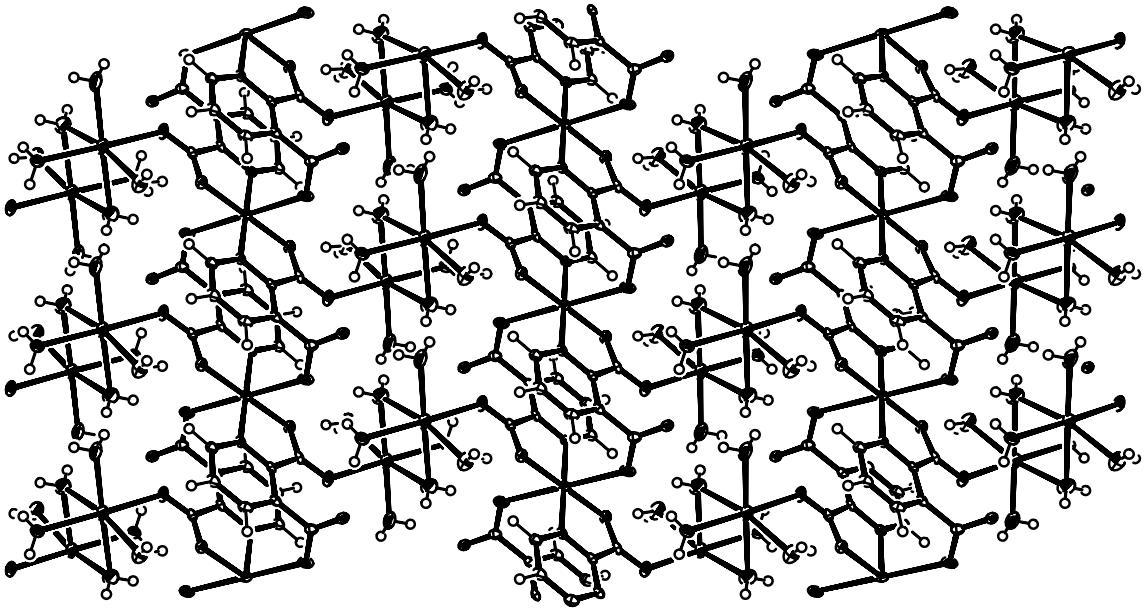

Fig. 7. View of a section of the polymeric sheet of **2**.

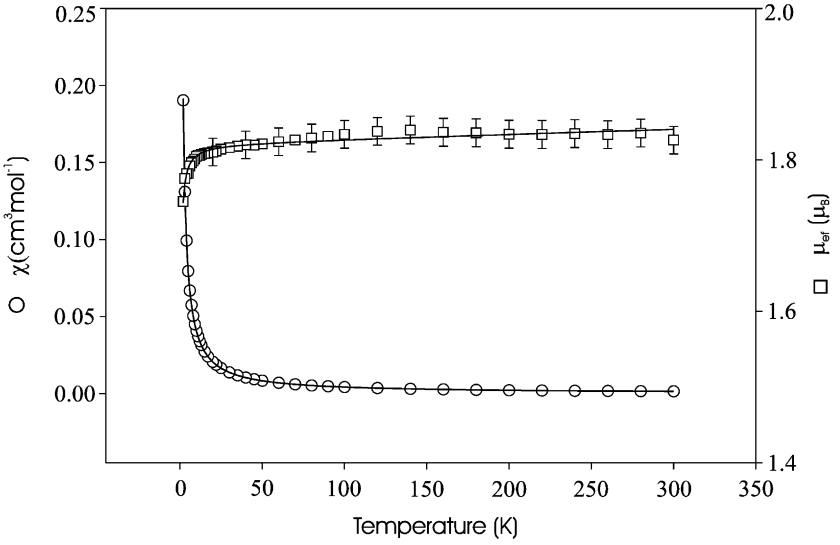

Fig. 8. χ_M and μ_{eff} vs. temperature plot for **2**, with error bars at ±0.5%. Lines are from theory as described in the text; the two equations used produced fits that are identical by inspection.

$J = -0.084(4)$ cm^{-1} and $g = 2.103(1)$, and a TIP correction of 0.000027(5) cm^3 mol^{-1}. These are consistent with the previously reported weak antiferromagnetic coupling fit to the Curie–Weiss law over the range 5–70 K [3]. A comparison of the Weng parameters of **1** and **2** shows the former to have a slightly larger coupling constant, with a difference more than seven times the esd. This is unexpected, given that most of the bonds relevant to the superexchange bridge are actually longer in the case of **2**. One possible explanation is that the disodium cations mediate a second dimension of antiferromagnetic superexchange; there is an instance in the literature of coordinated sodium ions forming part of a superexchange pathway [10]. The data were accordingly fit to the Lines model [11] for 2D antiferromagnetic exchange, achieving a satisfactory ($F = 0.005$) fit with the parameters $J = -0.123(6)$ cm^{-1} and $g = 2.103(1)$, and a TIP correction of 0.000029(5) cm^3 mol^{-1}. Due to differences in the way that the exchange coupling constants are defined, J values obtained from the Lines model [11] correspond to $2J$ from the Weng model [7,8]. In order to make a direct comparison between the two, it is therefore necessary to compare half of the Lines J value, i.e., −0.062 cm^{-1}, with the Weng J. This comparison shows that the Lines J for **2** is about six esd less than the Weng value for **2**, but is in excellent

agreement with the Weng value for **1**. Unfortunately, for such weak interactions it is not possible to conclude whether the exchange taking place in **2** is 1D or 2D. It is, however, clear that there is not much difference in the magnitude of exchange mediated by the bridging ligands in **1** and **2**.

3.3. $[Cu(2,3\text{-pydc})_2][Mn(H_2O)_6]\cdot 2H_2O$ (**3**)

Single-crystal X-ray studies reveal that **3** shares the same $[Cu(2,3\text{-pydc})_2]_n$ chain structure as **2** (see Fig. 9 for the repeat unit with atom labelling and Fig. 10 for a view of the polymeric structure). Like **2**, the bridging ligands are fully deprotonated; like **1** the polymeric structure is a single chain, in this case with the charge balanced by isolated $[Mn(H_2O)_6]^{2+}$ ions present in the lattice. Crystallographic data are given in Table 5, and selected bond lengths and angles are given in Table 6. In the crystal structure, there are two possible locations for the copper centre. Cu*a*, showing 70% occupancy, is in the same plane as the two pyridine rings; Cu*b*, showing 30% occupancy, is slightly displaced along the Cu–O4

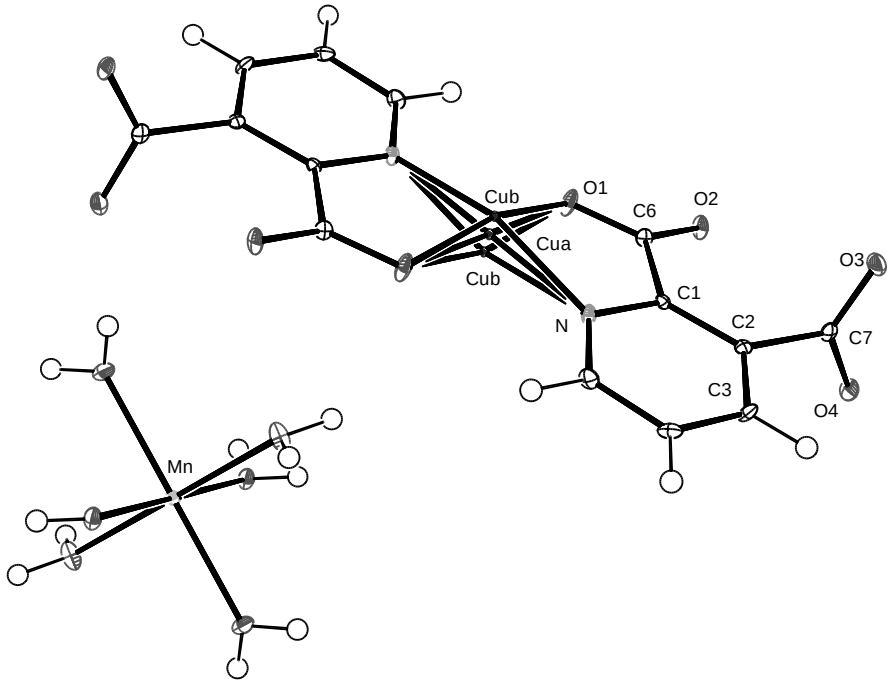

Fig. 9. Repeat unit of **3**, with atom labelling scheme and three possible locations for Cu^{2+} (50% ellipsoids).

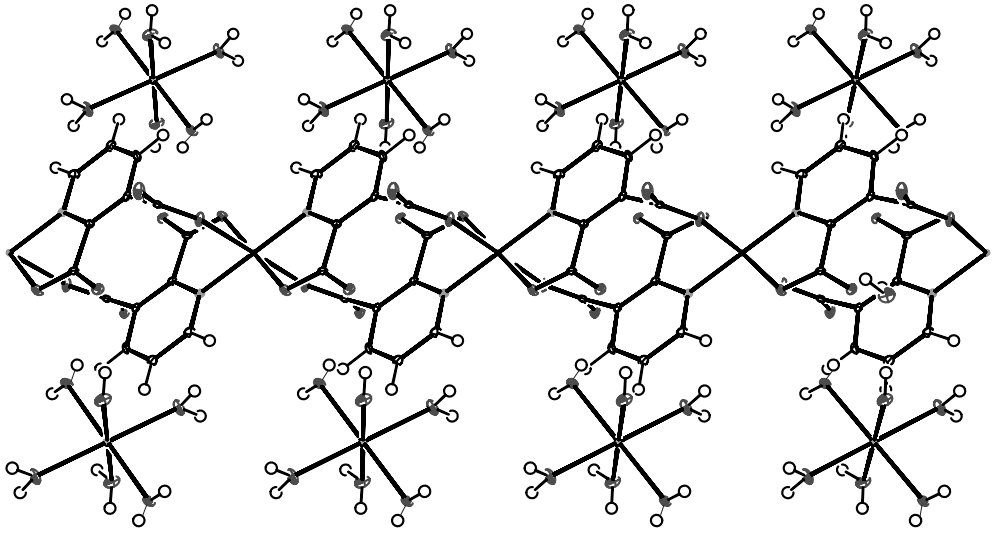

Fig. 10. View of a section of the polymeric chain of **3**, with adjacent $[Mn(H_2O)_6]^{2+}$ ions. Cu*b* has been omitted for clarity.

Table 5
Crytallographic data for **3**

Empirical formula	$C_{14}H_{22}N_2O_{16}CuMn$
Formula weight	592.82
Crystal system	triclinic
Space group	*P*1 (#2)
a (Å)	6.988(2)
b (Å)	7.5495(7)
c (Å)	11.253(1)
α (°)	85.420(3)
β (°)	72.523(3)
γ (°)	65.814(3)
V (Å^3)	515.9(1)
Z	1
ρ_{calc} (g cm^{-3})	1.91
μ(Mo Kα) (cm^{-1})	17.32
Crystal size (mm)	0.25 × 0.20 × 0.10
T (K)	173
$R(F)^*$	0.030
$R_W(F^2)^¥$	0.095
Number of parameters	188
Refinement	F^2

$^*R(F) = \sum ||F_o| - |F_c|| / \sum |F_o|$.
$^¥R_W(F^2) = (\sum(F_o^2 - F_c^2)^2 / \sum(F_o^2)^2)^{1/2}$.

Table 6
Selected bond lengths and distances (Å) and angles (°) for **3**

Bond lengths	
Cu*a*–N	1.942(2)
Cu*b*–N	1.900(2)/2.029(2)
Cu*a*–O1	1.962(1)
Cu*b*–O1	2.005(2)/1.966(2)
Cu*a*–O4	2.693(1)
Cu*b*–O4	2.390(3)/2.996(3)
Bond angles	
O1–Cu*a*–N	83.05(6)
O1–Cu*a*–O4	86.5(5)
Torsion angles	
C1–C2–C3–O1–C6–O2	8.13
C1–C2–C3–O3–C7–O4	77.28
Centroid–centroid distance (adjacent repeat units)	4.293
Ring plane–ring plane distance (adjacent repeat units)	3.409
Centroid–centroid to ring normal angle	37.43
Ring offset	2.609
O2–centroid distance	3.328

axis and may be either above or below the pyridine rings. Bond lengths are reported for Cu*a* and also for both the proximal and distal case of Cu*b*. In general, it may be said that the Cu–N bond is a little shorter in **3** than in **2**, which is in turn a little shorter than that in **1**; the Cu–O1 and Cu–O4 bonds follow the opposite trend. In the case of Cu*b*–O4, which is displaced along the Cu–O4 axis, the sum of the two reported bond lengths is equal to twice the Cu*a*–O4 bond length, suggesting that the spacing of repeat units is constant despite the 30% displacement of the Cu^{2+} ion. As in the other two structures, the pyridine rings of adjacent units lie parallel; in this case, with a centroid–centroid distance of 4.293 and an angle of 37.43° between the centroid–centroid and plane normal vectors, giving an offset of 2.609 Å. This is rather less than the offset in the previous two cases and the O2 of each group is less perfectly centred over the pyridine ring. As in **1**, the slight torsion of the 2-CO_2 group places O2 closer to the adjacent ring; the O2–centroid distance is 3.328 Å, compared to a distance of 3.409 Å between ring planes – once more a geometry suggestive of π–π interactions involving the carboxylate group [6]. As in **1**, an examination of the adjacent chains of **3** shows interchain π–π interactions; in this case, with a centroid–centroid distance of 3.345 Å and an angle of 21.09° between the centroid–centroid and ring normal vectors resulting in an offset of 1.204 Å, well within the range of slipped stacking π–π interactions examined by Janiak [6]. The water molecules ligating the Mn^{2+} ion and the lattice water all participate in hydrogen bonding, resulting in an extensive 3D H-bonding network stabilising the extended structure of **3**. Thermal analysis shows that H_2O is lost in two stages: four equivalents at 55 °C and the remaining four equivalents at 115 °C. Ligand decomposition occurs at 320 °C.

Interpretation of the magnetic susceptibility measurements for **3** (see Fig. 11 for susceptibility and moment plots) is complicated by the presence of two paramagnetic species. In analysing the data, it was assumed that the Mn^{2+} ions are magnetically dilute, and the data were fit to the sum of the previously used Weng model for Cu^{2+} and a Mn^{2+} zero-field splitting model modified from that described by O'Connor [12]. The equation used for Mn^{2+} was

$$\chi_m = \frac{1}{3}\left[C \times \frac{1 + 9e^{-2x} + 25e^{-6x}}{4(1 + e^{-2x} + e^{-6x})}\right] + \frac{2}{3}\left[\frac{9 + (8/2x)(1 - e^{-2x}) + (9/2x)(e^{-2x} - e^{-6x})}{4(1 + e^{-2x} + e^{-6x})}\right].$$

In order to get a reasonable fit, it proved necessary to consider the possible replacement of a portion of the copper centres by manganese. The data were therefore fit to an adjusted sum of the two models

$$\chi_m^{total} = a\chi_m^{Cu} + b\chi_m^{Mn},$$

where the coefficients *a* and *b* were used to model the replacement of some Cu^{2+} by Mn^{2+}. By setting *a* at 0.96 and *b* at 1.04, a 4% replacement of copper(II) by manganese(II), a satisfactory fit ($F = 0.007$) was obtained, with *g*(Mn) fixed at 2.00, TIP(Cu) fixed at 0.000100 cm^3 mol^{-1}, and the remaining parameters calculated to be $J(Cu) = -1.1$ (9) cm^{-1}, $g(Cu) = 2.25(3)$, and $D(Mn) = 0.5(1)$ cm^{-1}. The measured susceptibility is dominated by the paramagnetism of the Mn^{2+} centres; therefore the fit to the Weng model for Cu^{2+} has a large uncertainty

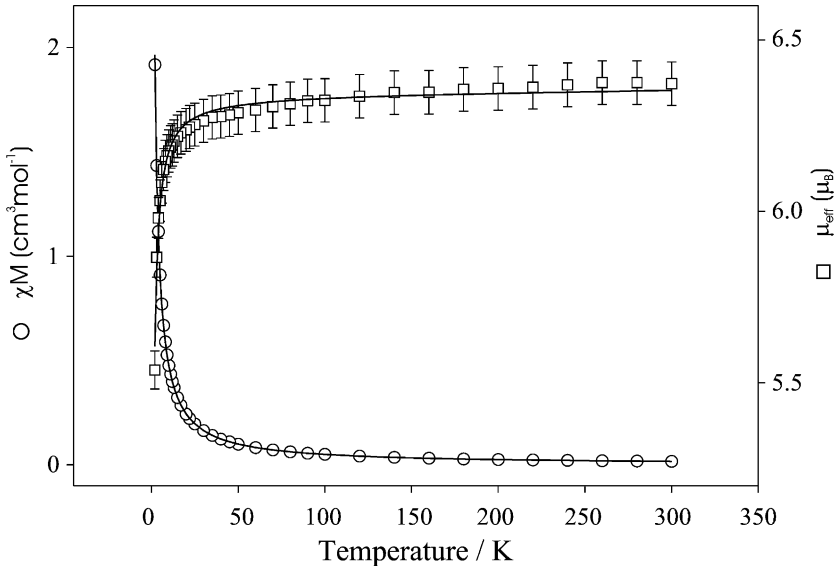

Fig. 11. χ_M and μ_{eff} vs. temperature plot for **3**, with error bars at ±0.5%. Lines are from theory as described in the text.

and generates a large esd in *J*. As a result, it is difficult to draw conclusions based on this *J*-value. Nonetheless, it is clear that weak 1D exchange is extent in **3**, and there is no evidence that the magnitude of this exchange is different from that observed in **1** and **2**.

4. Summary and conclusion

The chain structure of $[Cu(2,3\text{-pydcH})_2]$ (**1**), is very similar to that of the pyrazinedicarboxylate analogue $[Cu(2,3\text{-pyzdcH})_2]\cdot 2H_2O$ [1]. Given that one of the ring nitrogens in the latter compound is not involved in any coordinative interactions, this similitude is not surprising. Perhaps, more surprising is the fact that the long axial Cu–O interaction is a full 0.2 Å longer in **1** than in the corresponding pyrazinedicarboxylate compound. This structural feature is likely the main reason why the exchange coupling is weaker in **1** than in $[Cu(2,3\text{-pyzdcH})_2]$.

In preparing a fully deprotonated version of compound **1**, it was recognised that a structural analogue of the pyrazinedicarboxylate compound $[Cu(2,3\text{-pyzdc})(H_2O)_2]\cdot 2H_2O$ [1] was not possible. This latter compound has a chain structure in which each ring nitrogen is involved in a chelate interaction with a different copper centre [1], a bridging motif impossible for the pydc ligand with its single ring nitrogen to duplicate. Indeed, the fully deprotonated version of **1**, compound **2**, contains the same chain motif as **1** with the exception that the 3-carboxyl groups are deprotonated and charge neutrality is accomplished by the incorporation of a novel $[Na_2(H_2O)_6(\mu\text{-}H_2O)_2]^{2+}$ cation, which bridges the copper chains to generate an overall 2D sheet.

In order to investigate whether the sodium cations in **2** could be replaced by other metal ions, we reacted **2** with a salt of manganese(II) in water. The product from this reaction, **3**, retained the pydc bridged copper(II) chains, but replaced $[Na_2(H_2O)_6(\mu\text{-}H_2O)_2]^{2+}$with the hexaqua manganese(II) cation.

The persistence of the 2,3-pydc or 2,3-pydcH bridged copper chain motif in these three compounds requires further consideration. It seems likely that steric interactions between the two carboxylate groups in the adjacent 2,3-positions favour an orthogonal orientation between the two. Interestingly, in the pyrazine-2,3-dicarboxylate compound $[Cu(2,3\text{-pyzdc})(H_2O)_2]\cdot 2H_2O$, where both carboxylate moieties are involved in chelate interactions [1], the carboxylates do not adopt an orthogonal orientation but neither are they co-planar; the effects of steric repulsions between them are clearly observed. In **1, 2**, and **3**, with the orientation of the 2-carboxyl group fixed by the chelate interaction with one copper, the 3-carboxyl group rotates such that one of its oxygens is oriented favourably for the formation of the long axial bond to a neighbouring copper. The result is a chain structure in which the copper centres have the 4:2 geometry (four short bonds, two long) favoured by this Jahn–Teller ion.

In an examination of π–π stacking in metal complexes with nitrogen-containing aromatic ligands, based on a Cambridge Structural Database search, Janiak found that the usual π-interaction for pyridine type ligands is an offset or slipped stacking [6]. The data reveal that the vector between the ring centroids forms an angle of about 16°–40° with the ring normal, and that the centroid–centroid distance is 3.4 Å or greater, with a relative maximum number of examples around 3.8 Å. All three of the compounds reported here show intrachain slipped stacking of the pyridinedicarboxylate ligands in adjacent polymeric repeat units. The extent of slippage as measured by the centroid–centroid distances (4.2–4.6

Å) and displacement angles (37°–44°) places them at the extreme of those surveyed by Janiak [6]. In fact, this large slippage results in the 2-carboxyl groups lying, typically, directly above the centre of the neighbouring heterocyclic ring. This raises the possibility that π–π interactions involving the carboxylate groups contribute significantly to the stability of these polymers.

We also note that in **1** and **3**, the pyridinedicarboxylate ligands in adjacent chains also exhibit slipped stacking, with centroid–centroid distances (4.506 and 3.345 Å, respectively) and displacement angles (21.18° and 21.09°, respectively) also within the range surveyed by Janiak [6]. This evidence suggests that intrachain π-stacking, in this case without carboxyl group involvement, may also be a factor in stabilising these systems.

Hydrogen bonding is also present in all three compounds. In the case of **2** and **3**, an extensive 3D network of hydrogen bonds involving water molecules is observed. In the case of **1**, which is anhydrous, hydrogen bonding takes place between chains via the carboxylic acid proton, resulting in a novel 3D extended structure where one dimension is a coordinate-covalently bonded polymeric chain, the second undergoes π–π stacking interactions, and the third hydrogen bonding.

Finally, we note that the three compounds $[Cu(2,3\text{-}pyzdcH)_2]_x \cdot 2H_2O$, **1**, and **2** exhibit weak antiferromagnetic exchange with J values in the narrow range 0.05–0.1 cm^{-1}. The similarity in J is likely due to the similarity in the pathway for exchange in these three compounds and the weakness is likely due to the elongation of the axial Cu–O links in the pathway.

5. Supplementary material

Crystallographic data for the structural analysis have been deposited with the Cambridge Crystallographic Data Centre, CCDC No. 180987 for compound **1**, 180985 for compound **2**, and 180986 for compound **3**. Copies of this information may be obtained free of charge from the Director, CCDC, 12 Union Road, Cambridge, Cb2 1Ez, UK (fax: +44-1223-336033; e-mail: deposit@ccdc.cam.ac.uk or www.http://www.ccdc.cam.ac.uk).

Acknowledgements

R.C.T. and A.S. acknowledge the financial support of the Natural Sciences and Engineering Research Council of Canada. Elemental analyses were performed in the UBC Microanalysis Laboratory by P. Borda.

References

[1] L. Mao, S.J. Rettig, R.C. Thompson, J. Trotter, S. Xia, Can. J. Chem. 74 (1996) 433.
[2] C.J. O'Connor, C.L. Klein, R.J. Majeste, L.M. Trefonas, Inorg. Chem. 21 (1982) 64.
[3] E.E. Sileo, D. Vega, R. Baggio, M.T. Garland, M.A. Blesa, Aust. J. Chem. 52 (1999) 205.
[4] T. Suga, N. Okabe, Acta Cryst. C 52 (1996) 1410.
[5] M.K. Ehlert, S.J. Rettig, A. Storr, R.C. Thompson, J. Trotter, Can. J. Chem. 67 (1989) 1970.
[6] C. Janiak, J. Chem. Soc., Dalton Trans. (2000) 3885.
[7] W. Hiller, J. Strahle, A. Datz, M. Hanack, W.E. Hatfield, L.W.T. Haar, P. Gutlich, J. Am. Chem. Soc. 106 (1984) 329.
[8] C.-Y. Weng, Physics, Carnegie-Mellon, 1968, p. 157.
[9] A.J. Blake, C.M. Grant, S. Parsons, J.M. Rawson, G.A. Solan, R.E.P. Winpenny, J. Chem. Soc. Dalton Trans. (1995) 2311.
[10] G.D. Muno, D. Armentano, M. Julve, F. Lloret, R. Lescouezec, J. Faus, Inorg. Chem. 38 (1999) 2234.
[11] M.E. Lines, J. Phys. Chem. Solids 31 (1970) 101.
[12] C.J. O'Connor, Prog. Inorg. Chem. 29 (1982) 203.